Biochemical Pharmacology, Vol. 55, pp. 1843–1852, 1998.

ISSN 0006-2952/98/$19.00 + 0.00
PII S0006-2952(98)00070-7

Antioxidant and Cytoprotective Activities of the Calcium Channel Blocker Mibefradil

R. Preston Mason,‡§¶ I. Tong Mak,‖ Mary F. Walter,‡§ Thomas N. Tulenko† and Pamela E. Mason†‡*

Departments of *Biochemistry, †Physiology, and ‡Psychiatry, and §Center for Neurosciences Research, MCP ◆ Hahnemann School of Medicine, Allegheny University of the Health Sciences, Pittsburgh, PA 15212-4772; and ‖Departments of Medicine and Physiology, Division of Experimental Medicine, George Washington University Medical Center, Washington, DC 20037, U.S.A.

ABSTRACT. Mibefradil is a new calcium channel antagonist (CCA) that acts on both L- and T-type channels, with 10-fold selectivity for T-type channels. In this study, the structural interactions of mibefradil with cardiac membrane lipid bilayers were directly examined with small-angle x-ray diffraction approaches and correlated with lipid peroxidation and bovine aortic endothelial cell viability assays. Electron density profiles (Å vs electrons/Å^3) calculated from the diffraction data (37°C) demonstrated that mibefradil had an equilibrium location in the hydrocarbon core/headgroup region of the cardiac bilayer, 12–27Å from the center of the membrane. Mibefradil also effected a pronounced reduction in electron density 0–11Å from the center of the cardiac membrane concomitant with a 7.5% (3Å) decrease in membrane hydrocarbon core thickness; these changes in membrane structure were not observed with the phenylalkylamine verapamil, a CCA with some structural similarity to mibefradil. As a result of membrane physico-chemical interactions, mibefradil inhibited (10–500 nM) lipid peroxide formation in liposomes enriched in polyunsaturated fatty acids. In aortic endothelial cells, mibefradil also inhibited loss of cell viability (IC_{50} of 2 μM) following acute oxy-radical generation by dihydroxyfumarate and Fe-ADP; the order of potency was mibefradil > verapamil > diltiazem. These findings indicate that the chemical structure of mibefradil contributes to biophysical interactions with the cell membrane that underlie antioxidant and cytoprotective activities in models of oxidative stress. BIOCHEM PHARMACOL **55**;11:1843–1852, 1998. © 1998 Elsevier Science Inc.

KEY WORDS. calcium channel antagonists; lipid peroxidation; x-ray diffraction; endothelial cells

CCA** decrease vascular contractility and arterial tone by modulating the transmembrane influx of calcium into arterial smooth muscle cells [1]. The three classes of CCA that have been studied extensively are: 1,4-dihydropyridines, phenylalkylamines, and benzothiazepines, represented by nifedipine, verapamil, and diltiazem, respectively. Mibefradil is a chemically distinct (tetralol derivative) CCA that has been shown to inhibit inward L-type calcium currents in isolated cardiomyocytes [2] and also through T-type channels in vascular smooth muscle cells, with 10-fold selectivity for T-type channels [3]. The nonselective channel antagonist activity of mibefradil has been demonstrated in mammalian cells, in which mibefradil was able to inhibit, in a voltage-dependent manner, the calcium current through various α1 channel subunits (L-, N-Q-, and R-type) that were co-expressed with the α2/δ and β2b subunits [4]. Radioligand binding analyses in cardiac microsomes indicate that mibefradil interacts with a potentially unique location on the L-type calcium channel that overlaps the phenylalkylamine and benzothiazepine CCA binding sites, but not the DHP receptor site [5–8]. The nonselective modulation of calcium channels by mibefradil may be attributed to interactions of the antagonist with membrane sites on or near the protein.

In addition to its nonselective channel blocking properties, mibefradil is water-soluble and has an intrinsically long duration of activity [7]. The pharmacokinetic properties of mibefradil are similar to those reported for amlodipine, a highly amphipathic DHP that is extremely lipophilic ($K_p > 10^4$) as compared with verapamil, diltiazem, and several uncharged DHP analogs [9–11]. By way of comparison, the chemical properties of mibefradil may also cause it to partition to an energetically stable location in the membrane, resulting in extended equilibrium binding with membrane receptors [9]. Such strong affinity for the membrane lipid bilayer may also underlie *non*-receptor-mediated mechanisms of action for mibefradil, including the inhibition of free radical propagation in cells.

In this study, small-angle x-ray diffraction approaches

¶ Corresponding author: Dr. R. Preston Mason, Allegheny University of the Health Sciences, 320 E. North Avenue 10-ST, Pittsburgh, PA 15212-4772. Tel. (412) 359-4815; FAX (412) 359-6390; E-mail: mason@pgh.auhs.edu.

** *Abbreviations:* BCPC, bovine cardiac phosphatidylcholine; BHT, butylated hydroxytoluene; CCA, calcium channel antagonist(s); DHF, dihydroxyfumarate; DHP, 1,4-dihydropyridine; DLPC, dilinoleoyl phosphatidylcholine; and MTT, 3-(4,5-dimethylthiazol-2-yl)-2,5-diphenyl tetrazolium bromide.

Received 29 July 1997; accepted 5 January 1998.

were used to directly examine the membrane–structure interactions of mibefradil. The results of these analyses demonstrated that mibefradil intercalates into a region of high molecular density near the glycerol backbone/hydrocarbon core of the membrane. As a result of partitioning to this location in the membrane, mibefradil significantly altered membrane biophysical properties, resulting in an increase in molecular volume throughout a broad region of the membrane hydrocarbon core. The effects of mibefradil on the membrane provide a biophysical rationale for its potent antioxidant activity in liposomes, independent of calcium channel modulation. The cytoprotective activity of mibefradil was tested in cultured bovine aortic endothelial cells following acute oxy-radical generation from dihydroxyfumarate and Fe-ADP; mibefradil inhibited loss in endothelial cell viability in a concentration-dependent manner. Collectively, these findings provide additional insights into biophysical mechanisms of pharmacological inhibition of cellular oxidative damage.

MATERIALS AND METHODS

BCPC, DLPC, and cholesterol were purchased from Avanti Polar Lipids, Inc. and stored at −80°. The BCPC primary fatty acid composition was determined by gas–liquid chromatography to be as follows: 18:2 linoleic acid (30%), 16:0 palmitic acid (22%), 18:1 oleic acid (13%), 20:4 arachidonic acid (11%), and 20:3 homogamma linoleic acid (5%) (Avanti Polar Lipids, Inc.). Mibefradil (Ro 40-5967) was provided by F. Hoffmann–LaRoche, Ltd. Verapamil, nitrendipine, and diltiazem were purchased from RBI Biochemicals and stored in a desiccator at room temperature, protected from light.

Preparation of Membrane Vesicles for x-Ray Diffraction

Multilamellar vesicles consisting of cardiac phospholipid were prepared for x-ray diffraction experiments as previously described [12]. Cholesterol and phospholipid dissolved in chloroform at a 0.6:1 mole ratio were dried down with a stream of N_2 gas to a thin film on the sides and bottom of a 13 × 100-mm glass test tube while vortexing. Residual solvent was then removed by vacuum. For the x-ray diffraction experiments, buffer (0.5 mM of HEPES, 154.0 mM of NaCl, pH 7.2) was added to the dried lipid preparation, yielding a final phospholipid concentration of 5 mg/mL. Multilamellar vesicles were formed by vortexing the buffer and lipids for 3 min in the absence and presence of mibefradil or verapamil dissolved in buffer.

Preparation of Oriented Membrane Samples for x-Ray Diffraction

Oriented multilamellar membrane samples were prepared by centrifugation in Lucite sedimentation cells containing an aluminum foil substrate [13]. The samples were centrifuged in a Sorvall AH-629 swinging bucket ultracentrifuge rotor (DuPont) at 35,000 *g* for 1 hr at 5°. Upon completion of centrifugation, the supernatant was removed, and the "multibilayer" samples were mounted on curved glass supports. The samples were partially dehydrated overnight in glass vials containing a saturated salt solution ($ZnSO_4$) to define a specific relative humidity of 95% at 5°. The samples were then placed in sealed brass canisters in which temperature and relative humidity (93% relative humidity at 37°) were controlled.

Small-Angle x-Ray Diffraction Data Collection and Reduction

Small-angle x-ray diffraction studies were carried out by aligning the membrane multibilayers at near-grazing incidence with respect to the x-ray beam. The radiation source was a collimated, monochromatic x-ray beam (CuK_α x-ray, $\lambda = 1.54$Å) from a Rigaku RU-200 high-brilliance rotating anode x-ray generator (Rigaku USA). The experimental method utilized a single Franks' mirror defining a focused, nickel-filtered line source where $K_{\alpha 1}$ and $K_{\alpha 2}$ are unresolved.

Bragg's diffraction orders from the multilamellar samples were recorded on both a one-dimensional position-sensitive electronic detector (Innovative Technologies, Inc.) and a two-dimensional PhosphorImager system (Molecular Dynamics). Cholesterol monohydrate was used to verify the calibration. The sample-to-detector distance was 150 mm. The lamellar intensity functions from the oriented membrane samples were corrected using the Lorentz correction. A swelling analysis was used to assign unambiguous phases to the experimental structure factors [14].

Lipid Peroxidation Analyses

For these experiments, 500 μL of DLPC multilamellar vesicles (1.0 mg/mL) was freshly prepared in buffer (0.5 mM of HEPES, 154.0 mM of NaCl, pH 7.3) in the absence and presence of freshly prepared mibefradil, nitrendipine, verapamil, or diltiazem at various concentrations (10 nM through 500 nM). The vesicles were immediately placed in a shaking water bath at 37°. After a 24-hr incubation period, 100-μL aliquots of the samples were removed, and the peroxidation reaction was terminated by the addition of 25 μL of 5.0 mM of EDTA and 20 μL of 35.0 mM of BHT. The extent of lipid peroxidation in the samples was measured by the CHOD-Iodide assay [15]. The concentration of triiodide formed was measured spectrophotometrically.

$$LOOH + 2H^+ + 2I^- \rightarrow LOH + H_2O + I_2$$

$$I_2 + I^- \rightarrow I_3^-$$

To the above aliquot, 1.0 mL of CHOD color reagent was added, and the sample was allowed to incubate in the absence of light for 4 hr. The absorbance of the solution was then measured at 365 nm ($\varepsilon = 2.4 \times 10^4\ M^{-1}\ cm^{-1}$).

TABLE 1. Uncorrected normalized intensities for oriented cardiac membranes

Order No.	Control	Mibefradil		Verapamil	
		1% by mass	2% by mass	1% by mass	2% by mass
1	811,800 ± 21,840	893,600 ± 26,800	890,700 ± 24,700	860,500 ± 22,100	885,100 ± 22,810
2	106,400 ± 3,453	69,320 ± 1,672	71,210 ± 1,826	87,260 ± 2,687	67,540 ± 2,588
3	7,149 ± 934	2,197 ± 558	2,926 ± 310	3,759 ± 485	2,521 ± 300
4	72,930 ± 2,631	32,590 ± 822	31,920 ± 2,995	47,250 ± 1,640	42,730 ± 1,390
5	1,679 ± 407	2,296 ± 1,049	3,239 ± 624	1,240 ± 547	2,135 ± 573
	d = 55.7 Å	d = 53.5 Å	d = 52.0 Å	d = 54.8 Å	d = 53.9 Å

Experiments were carried out at 37°, 93% relative humidity. Values are means ± SD of three separate analyses.

Endothelial Cell Survival Assays

The cytoprotective activities of mibefradil, nifedipine, diltiazem, and verapamil were investigated in endothelial cells following oxy-radical production. Bovine aortic endothelial cells (GM 07372A) were obtained from the Coriell Institute for Medical Research and were cultured in Dulbecco's modified Eagle's medium supplemented with 10% calf serum. For subculturing, confluent plates were detached by 0.05% trypsin in 0.02% EDTA solution.

The index of endothelial cell survival was the colorimetric MTT assay according to the procedure of Mosmann [16], as described previously [17]. Trypsinized endothelial cells were seeded at a density of $1 \times 10^4/cm^2$ in Corning 24-well flat-bottomed tissue culture-treated plates in Dulbecco's modified Eagle's medium supplemented with 0.01 M of HEPES and 10% fetal bovine serum. After 24 hr of cell growth at 37° (cells in log phase), the medium was removed and replaced with 500 μL of the balanced salt buffer containing 10 mM of glucose, 125 mM of NaCl, 1.2 mM of $MgCl_2$, and 10 mM of potassium phosphate, pH 7.2. The attached cells were then incubated with or without the calcium antagonists for 30 min before exposure (except controls) to the iron-catalyzed free radical system consisting of 0.83 mM of DHF and 0.025 mM of $FeCl_3$ chelated by 0.25 mM of ADP for 30 min. With the concentration of free radical reagents used in the study, the rate of superoxide anions generated was 2.9 nmol/min/mL, measured by superoxide dismutase-inhibitable cytochrome *c* reduction. At the end of the free radical incubation period, all wells were replaced with the normal growth medium. At 24 hr post free radical exposure, all samples were quantitated for viable cells. Briefly, MTT, dissolved in PBS at 2 mg/mL, was added to all wells (125 μL/500 μL of medium), and then incubated for an additional 4 hr at 37°. Finally, 800 μL of acidified isopropanol (0.04 N of HCl in isopropanol) was added to all wells and mixed thoroughly with a pipette to dissolve the dark blue crystals. The supernatants were retrieved, briefly centrifuged, and read within 30 min using a test wavelength of 570 nm, and a reference of 700 nm.

RESULTS

Cardiac Membrane Bilayer x-Ray Diffraction Analysis

The molecular membrane interactions of mibefradil and verapamil were examined directly with small-angle x-ray diffraction techniques in cardiac membrane lipid bilayers. The cardiac lipid system was used in order to directly compare the interactions of mibefradil with other CCA that were examined previously by diffraction approaches [9–11]. x-Ray scattering from oriented cardiac membrane lipid bilayers consisting of >100 individual bilayers produced five strong, reproducible diffraction orders at 37° (Table 1). The unit cell periodicity or *d*-space (the measured distance from the center of one membrane to the next, including surface hydration) for the control cardiac membrane bilayer sample was 55.7 ± 0.3Å, while the intrabilayer headgroup separation was 40Å. In the presence of mibefradil (1% by mass), the cardiac membrane bilayer *d*-space was reduced to 53.5 ± 0.3Å, and the intrabilayer headgroup separation decreased by 2Å. At a higher concentration (2% by mass), the membrane *d*-space was reduced to 52.0 ± 0.3Å, and the intrabilayer headgroup separation decreased by 3Å or 7.5%.

Composite one-dimensional electron density profiles generated from the phased x-ray diffraction data indicated a centrosymmetric membrane bilayer structure (Fig. 1). The two peaks of electron density on either side of the figure correspond to phospholipid headgroups, while the minimum of electron density at the center of the membrane is associated with terminal methylene segments. The effects of mibefradil on membrane structure are demonstrated by directly subtracting the electron density profiles, as shown in Fig. 1.

The addition of mibefradil altered the structure of cardiac membrane lipid bilayers, as evidenced by changes in the one-dimensional electron density profiles. In the presence of mibefradil, there was an inward displacement of the phospholipid headgroups by 2Å and a broad decrease in electron density 0–11Å from the center of the membrane. At a higher concentration of mibefradil (2% by mass), the change in membrane structure was even more apparent, with a 3Å or 7.5% reduction in membrane hydrocarbon core width (Fig. 2A). In addition, the membrane *d*-space decreased to 52.0 ± 0.3Å in the presence of mibefradil (2% by mass). These changes in membrane structure are further evidence that the mibefradil molecule is strongly associated with the membrane, resulting in a perturbation of the intermolecular packing of phospholipid molecules.

The extent of the increase in membrane electron density 12–27Å from the center of the membrane (Fig. 1) is consistent with a molecular model that places the long axis

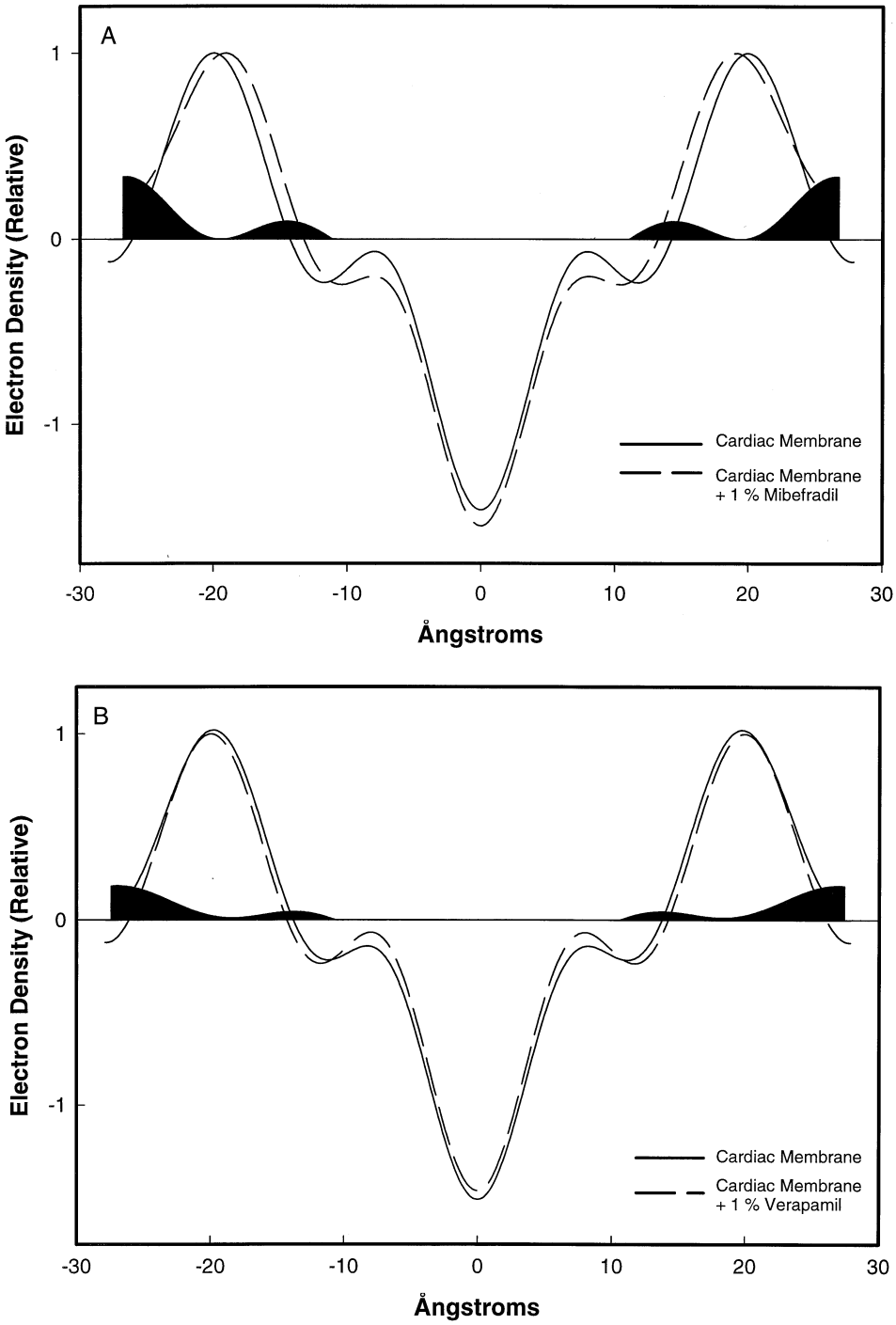

FIG. 1. Representative one-dimensional electron density profile (electrons/Å^3) of a centrosymmetric cardiac membrane lipid bilayer prepared in the absence and presence of (A) mibefradil (1% by mass) or (B) verapamil (1% by mass) at 37° and 93% relative humidity. The peaks of electron density correspond to the phospholipid headgroups, while the minimum of electron density at the center of the bilayer correlates with the terminal methylene segments, which have a relatively high hydrogen-to-carbon ratio. Positive differences in electron density (shaded regions) are attributed to the time-averaged molecular distribution of the drug compounds.

of mibefradil in an orientation that lies parallel to the phospholipid acyl chains. The mibefradil molecule extends from the upper acyl chains and glycerol backbone to the surface of the membrane. The fluorine substituent on the naphthyl group is particularly electron-dense and would serve as a strong scattering source for the x-rays in the hydrocarbon core region of the membrane. Verapamil, by contrast, has substantially less electron density in this same area of the membrane (12–19Å from the membrane center) (Fig. 1B). The location of the amphipathic mibefradil compound would facilitate electrostatic interactions (the pK_a values are 4.8 for the benzimidazolyl group and 5.5 for the tertiary amine), as well as hydrophobic interactions with the phospholipid acyl chains.

The addition of verapamil to cardiac membrane bilayers also produced discrete changes in the electron density profiles. Following the addition of verapamil (1% by mass), the membrane bilayer *d*-space was 54.8 ± 0.3Å, and the intrabilayer headgroup separation was 40Å (Fig. 1B). Direct subtraction of the control electron density profile from the

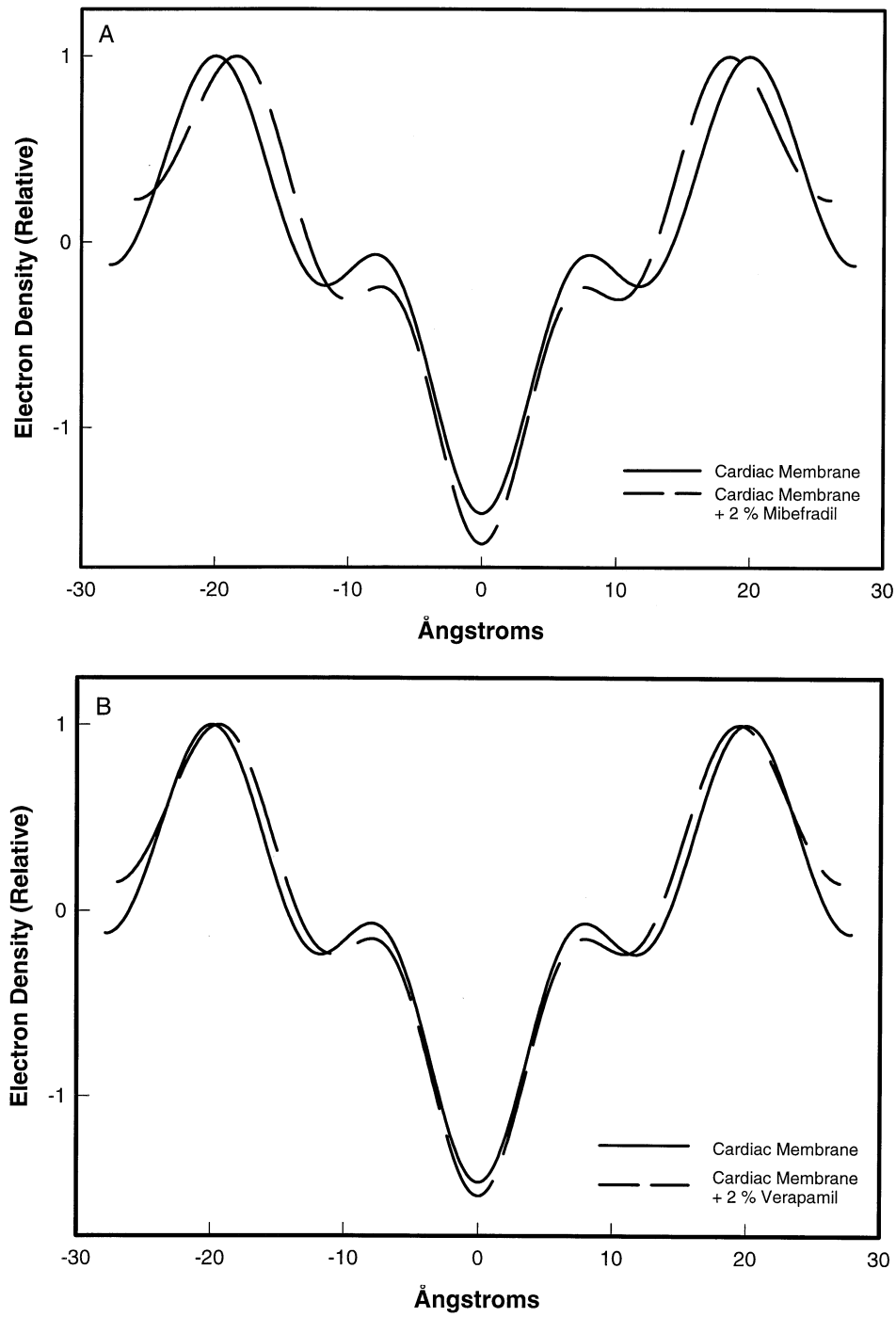

FIG. 2. Representative electron density profile (electrons/Å^3) of a centrosymmetric cardiac membrane lipid bilayer in the absence and presence of (A) mibefradil (2% by mass) or (B) verapamil (2% by mass) at 37° and 93% relative humidity. Under these conditions, a pronounced effect of mibefradil on the molecular structure of the membrane bilayer was demonstrated, including a reduction in hydrocarbon core width and molecular volume.

drug-containing sample showed an increase in electron density, 12–27Å from the center of the membrane. These data indicate that the verapamil molecule is also associated with the glycerol backbone/headgroup of the membrane but does not have the same effect on membrane structure as does mibefradil (Fig. 3–5).

Effect of CCA on Lipid Peroxidation

The antiperoxidant activity of mibefradil was evaluated in liposomes reconstituted from phospholipids enriched with DLPC, a polyunsaturated fatty acid (PUFA), at a 1.0 mg/mL concentration. DLPC vesicles were used to analyze the antioxidant activities of mibefradil and other CCA for the following reasons: (1) this system is well defined and highly reproducible, (2) linoleic acid is a common PUFA found in cardiac and vascular cell plasma membranes, (3) this membrane system does not contain calcium channels, and (4) lipid peroxidation in this system can be initiated spontaneously at 37° and does not require the addition of chemical initiators, such as iron-ascorbate. In these experiments, autoxidation occurred in a gradual, time-dependent

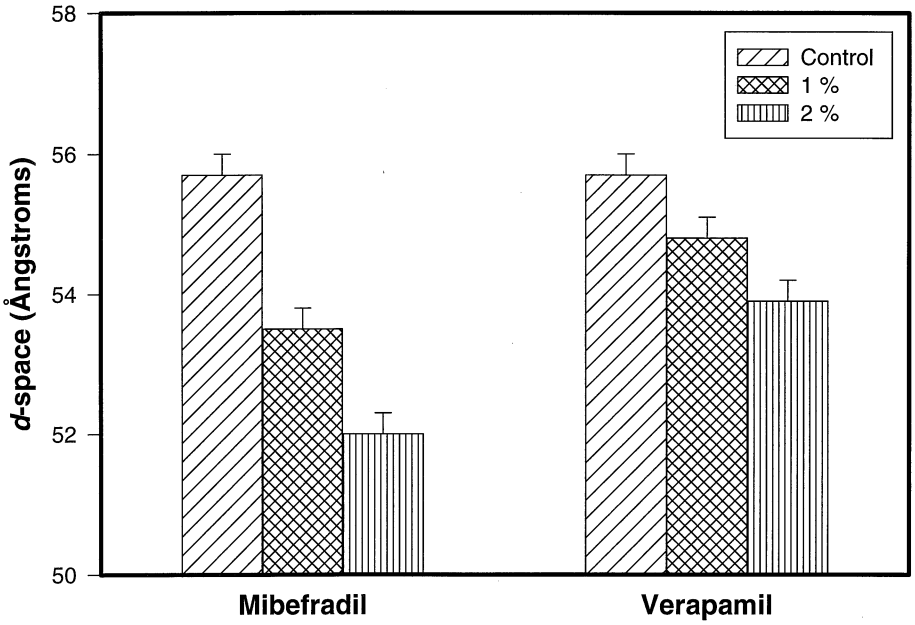

FIG. 3. Effect of mibefradil versus verapamil on the cardiac membrane lipid bilayer width at 37° and 93% relative humidity. The membrane *d*-space corresponds to the overall membrane bilayer width, including surface hydration. A reduction in membrane width is attributed to the intercalation of the drug molecule into the membrane hydrocarbon core, resulting in increased lateral separation of adjacent phospholipid molecules. These changes in membrane bilayer structure with mibefradil may contribute to its nonselective effect on calcium channel activity. The uncertainty in the membrane *d*-space measurements (±0.3Å) is due to instrumental error (means ± SD, based on at least 6 determinations).

manner that was measured spectrophotometrically; after a 24-hr incubation, the control vesicles had peroxidation levels that exceeded 550 μM. As demonstrated in Fig. 6, mibefradil inhibited lipid peroxidation in a time- and concentration-dependent manner. The antioxidant activity of mibefradil in this highly enriched PUFA system was potent: the mole ratio of mibefradil to linoleic acid was 1:26,000 at a 100-nM concentration.

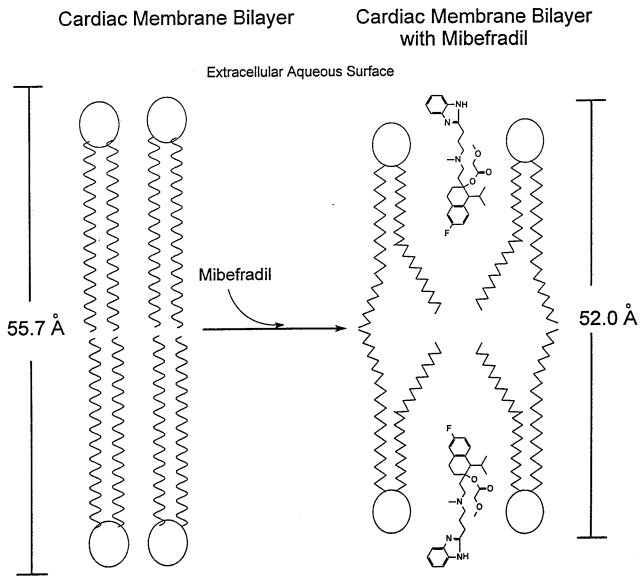

FIG. 4. Highly schematic illustration of the effect of mibefradil on cardiac membrane bilayer structure. As indicated by the x-ray diffraction data (Figs. 2 and 3), the presence of mibefradil in the membrane effects a reduction in membrane lipid bilayer width by altering the conformation of the phospholipid acyl chains.

Effect of CCA on Endothelial Cell Viability

The effect of free radical-induced cell injury was determined by cell growth assessment after treatment for 24 hr with the DHF-Fe oxy-radical system. Cell viability was assessed with the MTT assay that measures the conversion of the colorless tetrazolium salt (MTT) to the blue MTT formazan by the activity of mitochondrial dehydrogenase in living cells [16, 17]. With the seeding density employed, the control samples were in log phase for the entire period of the experiments; at 24 hr, the control samples exhibited about 60% confluence. Twenty-four hours after free radical exposure without drug treatment, the cell number decreased by 45 ± 5% with respect to the controls. Separate experiments were performed to confirm that the reduction in color products indeed corresponded to decreases in cell numbers. As shown in Fig. 7, mibefradil inhibited the loss of cell viability in a concentration-dependent manner with an IC_{50} of 2.0 μM following 24 hr of free radical treatment. At this 2.0-μM concentration, the potency of mibefradil was three-fold greater than that measured for verapamil (16% inhibition) and over five-fold greater than that for diltiazem (9% inhibition). Maximum protection by mibefradil was achieved by a 6.0-μM concentration (75%). It is important to note that at all the concentrations of mibefradil that were tested (1.0 through 20.0 μM), the drug had no effect on rates of free radical generation from the DHF-Fe system. Thus, the protective activity of mibefradil is attributed to its ability to attenuate free radical propagation in cell membranes.

DISCUSSION

The objective of this study was to examine the molecular interactions of mibefradil with cardiac membrane bilayers

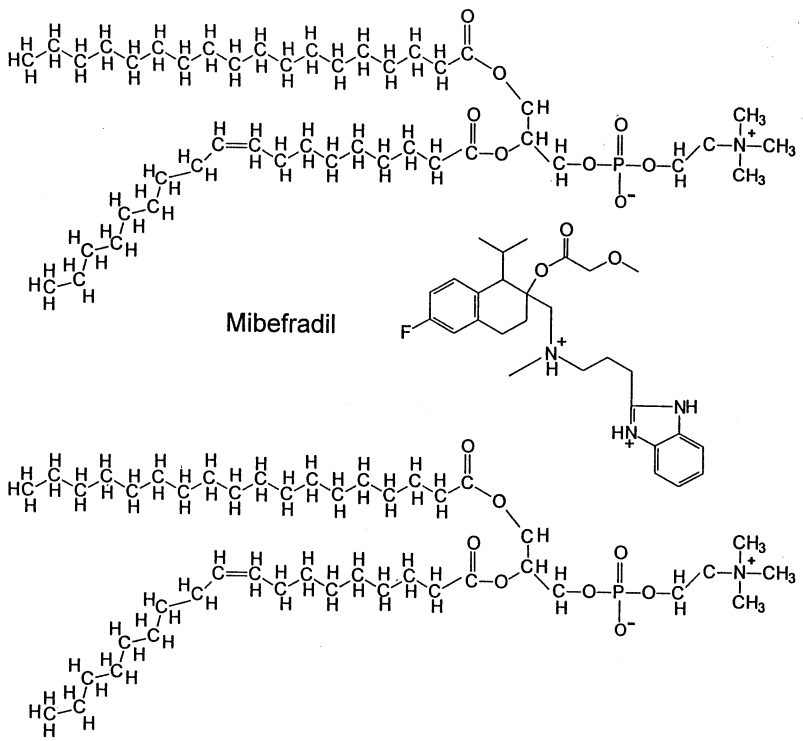

FIG. 5. Schematic illustration of molecular mibefradil/membrane interactions. Based on the x-ray diffraction analysis and known chemical properties of mibefradil, the following model is proposed. The location of the mibefradil is placed adjacent to a phospholipid molecule for reference with the benzimidazolyl group extending into the phospholipid headgroup region. The location of the amphipathic mibefradil molecule (the pK_a values are 4.8 for the benzimidazolyl group and 5.5 for the tertiary amine) would facilitate both hydrophobic and electrostatic interactions with neighboring phospholipid molecules.

and to correlate these interactions with antioxidant and cytoprotective activities following acute oxy-radical generation. The molecular location of mibefradil in cardiac membrane bilayers was ascertained with small-angle x-ray diffraction approaches. The results of these experiments demonstrated that mibefradil associates with the membrane and intercalates into the densely packed membrane hydrocarbon core/headgroup region. This well-defined membrane location for mibefradil was similar to that observed for verapamil (Figs. 1 and 2), a phenylalkylamine CCA that interacts with mibefradil at the L-type channel in a competitive manner [5, 7]. In addition, previous studies have shown that verapamil is lipophilic [10] and binds to a receptor site near the intracellular surface of the membrane [18]. The membrane location of mibefradil also overlaps that of diltiazem, as previously described for this cardiac membrane lipid bilayer system, but not the DHP, nisoldipine [19].

These structure data indicate a membrane site of interaction for mibefradil that is distinct from the membrane binding location previously observed for 1,4-dihydropyridines, deeper in the membrane hydrocarbon core [19–21], and as predicted from receptor binding data [6]. Interestingly, the charged 1,4-dihydropyridine amlodipine is different from other drugs in its class as it has a time-averaged location close to the membrane surface [9, 22]. The location of amlodipine allows it to interact with both the extracellular aqueous phase while it is bound to the L-type channel and with the receptor binding site of diltiazem, near the surface of the membrane [23, 24]. The membrane location for mibefradil would also facilitate both hydrophobic and electrostatic binding with neighboring phospholipid molecules, contributing directly to its intrinsically long duration of tissue activity by maintaining the drug in the lipophilic environment of its receptor(s), as previously described [7, 9, 21, 25]. A schematic model of the molecular interactions of mibefradil with adjacent phospholipid molecules is shown in Fig. 5.

These data demonstrate that the molecular distribution of mibefradil is 12–27Å from the center of the membrane bilayer, a region of high molecular density. The intercalation of mibefradil in this region of the membrane resulted in marked changes in phospholipid packing characteristics, as evidenced by an increase in the hydrocarbon core molecular volume 0–11Å from the center of the membrane as well as discrete reductions in membrane bilayer and hydrocarbon core widths by 4 and 3Å, respectively. These pronounced changes in phospholipid bilayer width are the result of acyl chain conformation changes (i.e. *trans-gauche* isomerizations), as previously described [26, 27]. Alterations in membrane structure as observed with mibefradil could be reproduced as a result of increasing acyl chain disorder by either decreasing membrane cholesterol content or increasing the membrane sample thermal energy [26, 27]. These structural effects of the mibefradil molecule on membrane bilayer width were concentration dependent and have not been observed for other CCA in this reconstituted cardiac lipid bilayer system [9, 11, 17].

The membrane interactions of mibefradil may contribute to its ability to modulate, in a nonselective fashion, various calcium channel types [4]. A previous study has demonstrated that changes in the structure of phospholipid molecules, as assessed by small-angle x-ray diffraction, have marked effects on the molecular kinetics of calcium-acti-

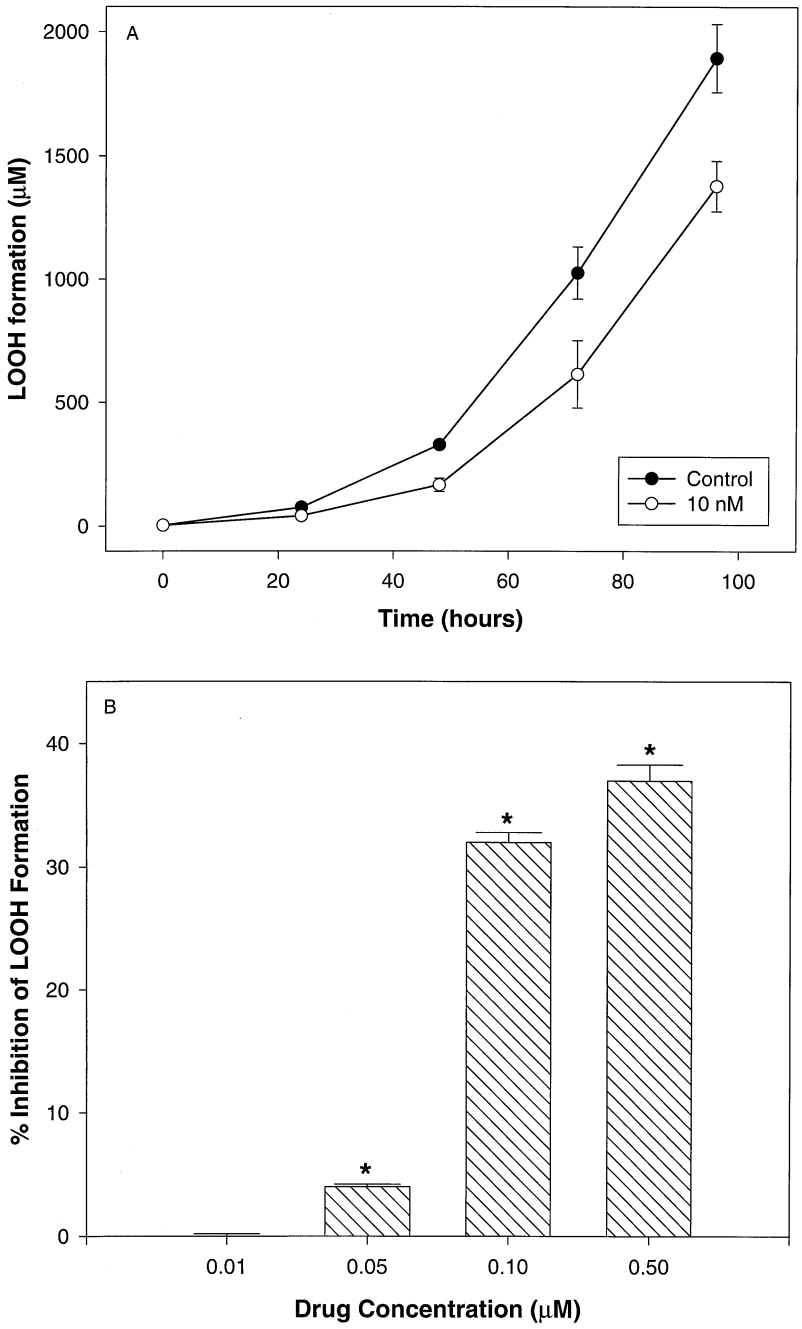

FIG. 6. (A) Time-dependent effect of mibefradil (10 nM) on lipid peroxide formation in DLPC vesicles (1.0 mg/mL) at 37°. Peroxide formation in either the presence or absence of drug was measured directly by spectrophotometric approaches at the indicated time points. (B) Concentration-dependent inhibition of membrane lipid peroxide formation by mibefradil (50.0 through 500.0 nM) after a 24-hr incubation period at 37°. Values are means ± SD, $N = 3$ (*$P < 0.01$, vs control).

vated potassium channels [28]. A reduction in membrane structural stress as a result of decreasing membrane cholesterol content (or increasing sample thermal energy) favored the open state of the channel by causing it to open more frequently [28]. Further electrophysiological studies are needed to address this hypothesis with mibefradil.

The distinct biophysical interactions of mibefradil with the membrane contributed to additional, non-receptor-mediated activities, as evidenced by its lipid antiperoxidant and cytoprotective activities in aortic endothelial cells (Figs. 6 and 7). Previous studies have shown that lipophilic CCA can attenuate the propagation of free radicals in cellular membranes, independent of specific receptor binding [29–31]. By intercalating into hydrophobic compartments of cellular membranes at concentrations that are several orders of magnitude higher than the surrounding aqueous environment [9–11], lipophilic CCA interfere with the propagation of free radicals through the membrane by various biophysical and biochemical mechanisms. In this study, mibefradil significantly reduced the amount of peroxide formation in liposomes enriched with polyunsaturated fatty acids in a concentration-dependent manner by inhibiting the propagation of free radicals. The activity of mibefradil was very potent; at a concentration of 100 nM, the ratio of mibefradil to linoleic acid molecules in these membrane preparations was approximately 1:26,000.

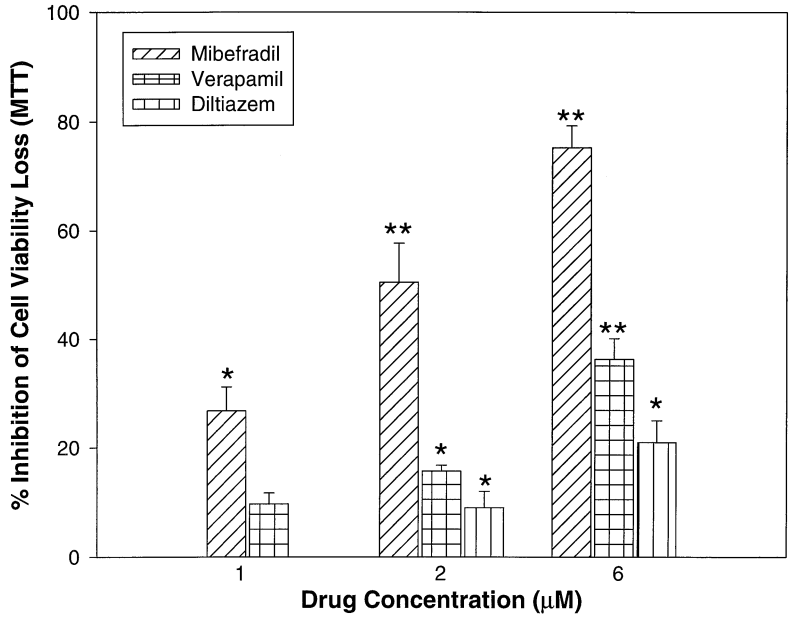

FIG. 7. Comparative protective effects of mibefradil, verapamil, and diltiazem against free radical-mediated loss of endothelial cell viability. The attached cells, 24 hr after seeding, were preincubated with each CCA at the indicated concentrations for 30 min before incubation with the free radical components (DHF + Fe-ADP) for 30 min. After 24 hr of incubation, cell viability was determined by the MTT assay, as described in Materials and Methods. Values are means ± SD of 3–4 separate determinations (*$P < 0.05$ and **$P < 0.01$, vs control).

The antiperoxidant activity of mibefradil in this system is attributed primarily to its pronounced effects on membrane biophysical properties, as described above. By significantly altering the intermolecular packing and structure of membrane lipid constituents, mibefradil can interfere with the diffusion of highly unstable free radicals through the membrane hydrocarbon core, independent of calcium channel modulation. This intriguing model is consistent with a previous study which demonstrated that physical conditions (i.e. temperature) and lipid composition (i.e. cholesterol content) that affect the packing density of fatty acids can dramatically alter rates of membrane lipid peroxidation [32]. In addition to modulating membrane biophysical properties, mibefradil may also attenuate rates of lipid peroxidation by radical-resonating mechanisms due to its conjugated ring structure located in the membrane hydrocarbon core (Fig. 5). These findings provide new insights into the relationship between rates of lipid peroxidation and membrane structure modulation by a pharmacological agent.

The membrane antioxidant properties of mibefradil appear to contribute to cytoprotective activity in an endothelial cell model of survival following acute oxy-radical generation. In the vascular wall, oxygen free radicals can be produced endogenously from activated neutrophils, macrophages, autoxidizing catecholamines, and redox active drugs, leading to tissue injury. The results from this study indicate that mibefradil had potent cytoprotective activity, as compared with other CCA analogs. At all the concentrations of mibefradil that were tested (1.0 through 20.0 μM), the drug had no effect on the rates of free radical generation from the DHF-Fe system; the protective activity of mibefradil is attributed, therefore, to its ability to attenuate the propagation of free radicals in cellular membranes. Collectively, these findings indicate that modulation of membrane biophysical properties by mibefradil contribute to antioxidant properties that may have pharmacological relevance in various models of chronic (atherosclerosis) and acute (ischemia-reperfusion) tissue injury resulting from free radical-mediated damage.

The investigators acknowledge research support from the Allegheny-Singer Research Institute and the National Institutes of Health, and from F. Hoffmann–LaRoche, Ltd., which provided mibefradil for this study. The authors wish to express their appreciation to Drs. Henry Solomon and Jean-Paul Clozel for helpful scientific discussions related to this study.

References

1. Janis RA, Silver PJ and Triggle DJ, Drug action and calcium regulation. *Adv Drug Res* **16:** 309–591, 1987.
2. Fang L-M and Osterrieder W, Potential-dependent inhibition of cardiac Ca^{2+} inward currents by Ro 40-5967 and verapamil: Relation to negative inotropy. *Eur J Pharmacol* **196:** 205–207, 1991.
3. Mishra SK and Hermsmeyer K, Selective inhibition of T-type Ca^{2+} channels by Ro 40-5967. *Circ Res* **75:** 144–148, 1994.
4. Bezprozvanny I and Tsien RW, Voltage-dependent blockade of diverse types of voltage-gated Ca^{2+} channels expressed in *Xenopus* oocytes by the Ca^{2+} channel antagonist mibefradil (Ro 40-5967). *Mol Pharmacol* **48:** 540–549, 1995.
5. Osterrieder W and Holck M, *In vitro* pharmacologic profile of Ro 40-5967, a novel Ca^{2+} channel blocker with potent vasodilator but weak inotropic action. *J Cardiovasc Pharmacol* **13:** 754–759, 1989.
6. Rutledge A and Triggle DJ, The binding interactions of Ro 40-5967 at the L-type Ca^{2+} channel in cardiac tissue. *Eur J Pharmacol* **280:** 155–158, 1995.
7. Clozel J-P, Osterrieder W, Kleinbloesem CH, Welker HA, Schlappi B, Tudor R, Hefti F, Schmitt R and Eggers H, Ro 40-5967: A new nondihydropyridine calcium antagonist. *Cardiovasc Drug Rev* **9:** 4–17, 1991.
8. Orito K, Satoh K and Taira N, Cardiovascular profile of Ro 40-5967, a new nondihydropyridine calcium antagonist, de-

lineated in isolated, blood-perfused dog hearts. *J Cardiovasc Pharmacol* **22:** 293–299, 1993.
9. Mason RP, Campbell SF, Wang S-D and Herbette LG, Comparison of location and binding for the positively charged 1,4-dihydropyridine calcium channel antagonist amlodipine with uncharged drugs of this class in cardiac membranes. *Mol Pharmacol* **36:** 634–640, 1989.
10. Mason RP, Moisey DM and Shajenko L, Cholesterol alters the binding of Ca^{2+} channel blockers to the membrane lipid bilayer. *Mol Pharmacol* **41:** 315–321, 1992.
11. Mason RP, Gonye GE, Chester DW and Herbette LG, Partitioning and location of Bay K 8644, 1,4-dihydropyridine calcium channel agonist, in model and biological membranes. *Biophys J* **55:** 769–778, 1989.
12. Bangham AD, Standish MM and Watkins JC, Diffusion of univalent ions across the lamellae of swollen phospholipids. *J Mol Biol* **13:** 238–252, 1965.
13. Herbette L, DeFoor P, Fleischer S, Pascolini D, Scarpa A and Blasie JK, The separate profile structures of the functional calcium pump protein and the phospholipid bilayer within isolated sarcoplasmic reticulum membranes determined by X-ray and neutron diffraction. *Biochim Biophys Acta* **817:** 103–122, 1985.
14. Moody MF, X-ray diffraction pattern of nerve myelin: A method for determining the phases. *Science* **142:** 1173–1174, 1963.
15. El-Saadani M, Esterbauer H, El-Sayed M, Goher M, Nassar AY and Jurgens G, A spectrophotometric assay for lipid peroxides in serum lipoproteins using a commercially available reagent. *J Lipid Res* **30:** 627–630, 1989.
16. Mosmann T, Rapid colorimetric assay for cellular growth and survival: Application to proliferation and cytotoxicity assays. *J Immunol Methods* **65:** 55–63, 1983.
17. Mak IT, Boehme P and Weglicki WB, Protective effects of calcium channel blockers against free radical-impaired endothelial cell proliferation. *Biochem Pharmacol* **50:** 1531–1534, 1995.
18. Hescheler J, Pelzer D, Trube G and Trautwein W, Does the organic calcium channel blocker D600 act from inside or outside the cardiac cell membrane? *Eur J Physiol* **393:** 287–291, 1982.
19. Mason RP and Trumbore MW, Differential membrane interactions of calcium channel blockers: Implications for antioxidant activity. *Biochem Pharmacol* **51:** 653–660, 1996.
20. Baindur N, Rutledge A and Triggle DJ, A homologous series of permanently charged 1,4-dihydropyridines: Novel probes designed to localize drug binding sites on ion channels. *J Med Chem* **36:** 3743–3745, 1993.
21. Bangalore R, Baindur N, Rutledge A, Triggle DJ and Kass RS, L-Type calcium channels: Asymmetrical intramembrane binding domain revealed by variable length, permanently charged 1,4-dihydropyridines. *Mol Pharmacol* **46:** 660–666, 1994.
22. Bauerle H-D and Seelig J, Interaction of charged and uncharged calcium channel antagonists with phospholipid membranes. Binding equilibrium, binding enthalpy, and membrane location. *Biochemistry* **30:** 7203–7211, 1991.
23. Kass RS and Arena JP, Influence of pH on calcium channel block by amlodipine, a charged dihydropyridine compound: Implications for location of the dihydropyridine receptor. *J Gen Physiol* **93:** 1109–1127, 1989.
24. Rigby JW, Gardiner DG, Greengrass PM and Burges RA, Amlodipine: Interaction with calcium channel binding sites. *J Cardiovasc Pharmacol* **12:** S144, 1988.
25. Rhodes DG, Sarmiento JG and Herbette LG, Kinetics of binding of membrane-active drugs to receptor sites: Diffusion-limited rates for a membrane bilayer approach of 1,4-dihydropyridine Ca^{2+} channel antagonists to their active site. *Mol Pharmacol* **27:** 612–23, 1985.
26. Chen M, Mason RP and Tulenko TN, Atherosclerosis alters the composition, structure and function of arterial smooth muscle cell plasma membranes. *Biochim Biophys Acta* **1272:** 101–112, 1995.
27. Mason RP, Trumbore MW and Pettegrew JW, Membrane interactions of a phosphomonoester elevated early in Alzheimer's disease. *Neurobiol Aging* **16:** 531–539, 1995.
28. Chang HM, Reitstette R, Mason RP and Gruener R, Attenuation of channel kinetics and conductance by cholesterol: An interpretation using structural stress as a unifying concept. *J Membr Biol* **143:** 51–63, 1995.
29. Mak IT and Weglicki WB, Comparative antioxidant activities of propranolol, nifedipine, verapamil, and diltiazem against sarcolemmal membrane lipid peroxidation. *Circ Res* **66:** 1449–1452, 1990.
30. Mak IT, Boehme P and Weglicki WB, Antioxidant effects of calcium channel blockers against free radical injury in endothelial cells. Correlation of protection with preservation of glutathione levels. *Circ Res* **70:** 1099–1103, 1992.
31. Janero DR and Burghardt B, Antiperoxidant effects of dihydropyridine calcium antagonists. *Biochem Pharmacol* **38:** 4344–4348, 1989.
32. McLean LR and Hagaman KA, Effect of lipid physical state on the rate of peroxidation of liposomes. *Free Radic Biol Med* **12:** 113–119, 1992.